


Active Hard Spheres in Infinitely Many Dimensions

Thibaut Arnoult de Pirey,¹ Gustavo Lozano², and Frédéric van Wijland¹

¹*Université de Paris, Laboratoire Matière et Systèmes Complexes (MSC), UMR 7057 CNRS, F-75205 Paris, France*

²*Departamento de Física, Facultad de Ciencias Exactas y Naturales, Universidad de Buenos Aires, Ciudad Universitaria, Pabellón I, 1428 Buenos Aires, Argentina*

 (Received 5 October 2019; published 26 December 2019)

Few equilibrium—even less so nonequilibrium—statistical-mechanical models with continuous degrees of freedom can be solved exactly. Classical hard spheres in infinitely many space dimensions are a notable exception. We show that, even without resorting to a Boltzmann distribution, dimensionality is a powerful organizing device for exploring the stationary properties of active hard spheres evolving far from equilibrium. In infinite dimensions, we exactly compute the stationary state properties that govern and characterize the collective behavior of active hard spheres: the structure factor and the equation of state for the pressure. In turn, this allows us to account for motility-induced phase separation. Finally, we determine the crowding density at which the effective propulsion of a particle vanishes.

DOI: [10.1103/PhysRevLett.123.260602](https://doi.org/10.1103/PhysRevLett.123.260602)

Understanding the collective behavior of simple liquids has been a fundamental statistical mechanical challenge since its early days [1]. The absence of a well-defined and versatile approximation method able to capture collective effects in liquids has led to the development of a branch in its own right: the art of elaborating approximations leading to correlations in fluids is almost as old as statistical mechanics itself [2,3]. It was only in the mid-eighties that Frisch, Rivier, and Wyler [4] were able to devise a bona fide mean-field approximation. The latter takes the form of a controlled large dimensionality limit in which they could derive, among other thermodynamical properties, an exact equation of state for classical hard spheres. The physical price to pay by going to large space dimensions is heftily compensated by the mathematical gain: not only the equation of state [4,5], but also thermodynamic quantities, such as the entropy [6] and even transport coefficients inferred from the collision dynamics [7] can be determined exactly. Perhaps more importantly, the greatest insight is to be found in the pair-correlation function in that it, alone, controls the spatial organization of the fluid [8], and, thus, can be used as an educated starting point for density functional approaches [9] (see [10] for a recent overview).

The realization that classical infinite-dimensional hard spheres lent themselves to analytical treatment, especially regarding the determination of entropy, laid the ground for the idea that they could also be used to investigate metastability issues (understood in terms of free energy minima) [11–13]. Thus, they have become the workhorse of the theory of jamming and of the static approach to glasses. More recent inroads into dynamical behavior [14–17] address relaxation properties, including with nonequilibrium evolutions [18]. For some of these glassy-behavior-related questions, the high dimensionality comes with its

own share of hotly debated issues as to what exactly survives finite dimensions [19]. A pivotal starting point common to all static approaches is the celebrated equilibrium Boltzmann weight. In stark contrast, no such shortcut exists for the stationary properties of active matter systems, and thus, it is no surprise that a many-body exactly solvable model of particles interacting with pairwise forces has, so far, remained elusive. In active systems, the motion of the individual particles requires a net consumption of energy taken from the environment [20–22]. Breaking the delicate balance between dissipation and injection of energy at the particle level inevitably drives even the simplest versions of such interacting particle systems away from equilibrium. Among microscopic models ubiquitous in the active matter literature, the simplest ones involve overdamped dynamics in the presence of a self-propulsion force, the statistics of which strongly deviate from the Gaussian white noise familiar in equilibrium. For such systems, even with short-range repulsive interactions, the possibility of a phase separation into a coexisting dense phase and a dilute one is a direct consequence of the genuine nonequilibrium character of the dynamics. This so-called motility-induced phase separation (MIPS) occurs when the typical run length due to self-propulsion notably exceeds the range of repulsive interactions. MIPS is a phenomenon that has received considerable attention [23–25], as it is probably the simplest activity-driven emerging collective phenomenon. Understanding collective behavior in active matter combines the hurdles of strongly correlated liquids with those of nonequilibrium physics. Our purpose is to show how working in infinite dimension allows us to overcome both, and to eventually bridge the microscopic behavior to the macroscopics. In this Letter, we begin by defining the proper infinite-dimensional scalings of the model parameters so as

to maintain a competition between activity and repulsive pairwise interactions leading to a complex spatial organization. Then, we solve the two-body problem and use our result to explain how working in large dimension allows us to truncate the hierarchy of correlations to second order. Relevant physical quantities are then explicitly derived. The effective propulsion velocity [26] is shown to vanish linearly at a crowding density which we identify. The equation of state [27] for the homogenous phase exhibits a regime of negative compressibility that signals the MIPS spinodal, the shape of which is also found exactly.

Our starting point for the dynamics of each particle is an overdamped equation of motion for its position $\mathbf{r}_i(t)$

$$\frac{d\mathbf{r}_i}{dt} = -\sum_{j \neq i} \partial_{\mathbf{r}_i} V(\mathbf{r}_i - \mathbf{r}_j) + v_0 \mathbf{u}_i, \quad (1)$$

where the particle's mobility has been set to unity for convenience, $V(\mathbf{r})$ is the interaction potential between two particles, v_0 is a self-propulsion velocity scale, while \mathbf{u}_i is a random orientation vector. A variety of models enter this schematic description: for the run-and-tumble particles (RTPs) we consider here, \mathbf{u}_i is a unit vector that picks a random direction at rate τ^{-1} (but, as we discuss in [28], our conclusions extend to active Brownian [29] and active Ornstein-Uhlenbeck [30] particles). Throughout, the potential V , we have in mind is a smooth repulsive potential of the form $V(r) = V_0 \exp\{-[d(r - \sigma)/\sigma\epsilon]\}$ where the d factor keeps it short ranged in the large-dimensional limit [31], and where $\epsilon \rightarrow 0^+$ further allows us to take a hard-sphere limit of diameter σ . The run length between two tumbles $\ell = v_0\tau$ and the particle density ρ are the other two dimensional quantities entering our problem. For non-interacting RTPs the diffusion constant is $(v_0^2\tau/d)$ and we choose, as $d \rightarrow \infty$, to keep it fixed. We choose to work at fixed persistence time τ which leads to keeping $\hat{v}_0 = v_0/\sqrt{d}$ fixed. Thus, the limit of interest is one of a highly ballistic nature where $\ell = \hat{v}_0\tau\sqrt{d} \gg \sigma$ (i.e., of very large persistence length to particle size ratio $v_0\tau/\sigma$). While other scalings maintaining the nonequilibrium nature of the dynamics are possible (see [28]), this is the only one yielding a phenomenology of collective effects such as MIPS similar to that of lower dimensional systems. By contrast, the equilibrium limit, while keeping the diffusion constant fixed as well, requires working at a persistence length vanishingly small with respect to any other relevant scale. Sending $d \rightarrow \infty$ first and then $\tau \rightarrow 0$ does not allow us, here, to recover the equilibrium phenomenology. As in [4,11,13,32], we work at density scales such that $\rho V_d(\sigma) \sim O(d)$, so that a given particle typically has d neighbors [here, $V_d(\sigma)$ is the exclusion volume of a particle], hence, leaving room for nontrivial collective behavior. Therefore, potential gradients are also endowed with a characteristic scale, as we show now. During a

collision event between two particles, their relative velocity along the direction of the collision vanishes. The latter features three contributions. The first one accounts for self-propulsion and is of order v_0/\sqrt{d} due to the randomization of the \mathbf{u}_i 's. The second is the two-particle direct interaction of order $\partial_r V$, and the third one contains collisions with the rest of the particles: it is a sum over d random contributions (that, for now, we assume to be weakly correlated), each of them being of order $\partial_r V/\sqrt{d}$, hence, a global contribution of order $\partial_r V$ as well. Thus, altogether, we expect that $\partial_r V$ is of order \hat{v}_0 .

Now, let us discuss the picture that emerges at $d \gg 1$ for just two particles, which amounts to considering the motion of the relative particle with orientation $\mathbf{u} = \mathbf{u}_2 - \mathbf{u}_1$ around a fixed spherical obstacle. The impact parameter is given by $b = r \sin \theta$ ($r = \|\mathbf{r}\|$) as depicted in Fig. 1, but we anticipate that the typical values of interest for θ are such that $\cos^2 \theta \sim d^{-1}$ due to the randomization of \mathbf{u} . The relative motion of an incoming particle a distance $r = \sigma + \delta r$ away from this spherical obstacle is unaffected by the obstacle unless $\delta r/\sigma = O(1/d)$. Indeed, if $\delta r/\sigma = O(1)$, a collision event can occur if and only if $\cos \theta = O(1)$, which is exponentially rare in d . When a flip does occur, $\delta r/\sigma$ will remain at least of $O(1)$ so that the particle typically misses the obstacle again. Down to these scales, the obstacle is invisible and the particle undergoes a free run-and-tumble motion. This means the density is uniform up to distances $\delta r/\sigma \sim O(1)$. If, however, $\delta r/\sigma$ becomes $O(d^{-1})$ the probability that \mathbf{u} points towards the obstacle is not negligible anymore so that collision events potentially shape a nontrivial density profile around the obstacle over a scale $\delta r \sim \sigma/d$. We justify this by computing $g_0(\mathbf{0}, \mathbf{r}; \mathbf{u}_1, \mathbf{u}_2)$, the two-point function of the two-body

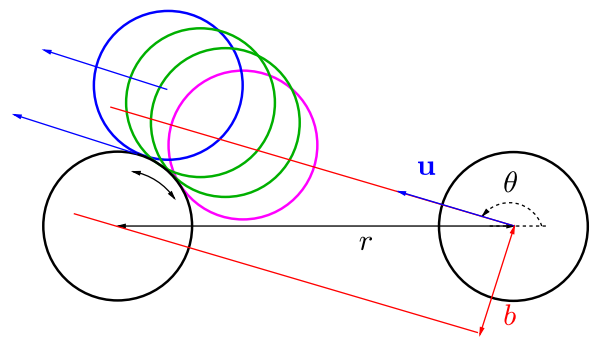


FIG. 1. A collision of an active hard sphere (black, rightmost) with diameter σ and impact parameter $b = r \sin \theta < \sigma$ (and $\cos \theta < 0$) onto a pinned (black, leftmost) one. The incoming particle with direction \mathbf{u} hits the target sphere (at the magenta position) and then skids around by occupying the sequence of green positions. It eventually takes off at the blue position when its orientation \mathbf{u} becomes tangent to the target sphere. No tumble can occur over the typical skidding distances considered here, which are of order σ/\sqrt{d} .

problem for having a particle at 0 with orientation \mathbf{u}_1 and a particle at \mathbf{r} with orientation \mathbf{u}_2 . The equation for g_0 reads

$$-v_0(\mathbf{u}_2 - \mathbf{u}_1) \cdot \nabla_{\mathbf{r}} g_0 + 2\nabla_{\mathbf{r}} \cdot [g_0 \nabla_{\mathbf{r}} V(\mathbf{r})] + \mathcal{R}g_0 = 0, \quad (2)$$

where \mathcal{R} is a linear operator acting on g_0 and accounting for the dynamics of \mathbf{u}_1 and \mathbf{u}_2 which occurs at a rate $1/\tau$. A stimulating inspiration for the solution of Eq. (2) comes from the one-dimensional cases of two particles on a ring [33], or of one particle between two hard walls [34] where density profiles exhibit delta peak contributions. In the hard-sphere limit of Eq. (2), as we show in [28], this also holds in arbitrary dimension d where $g_0(\mathbf{0}, \mathbf{r}; \mathbf{u}_1, \mathbf{u}_2)$ takes the form

$$g_0(\mathbf{0}, \mathbf{r}; \mathbf{u}_1, \mathbf{u}_2) = f(\mathbf{r}; \mathbf{u}_1, \mathbf{u}_2)\theta(r - \sigma) + \Gamma(\hat{\mathbf{r}}; \mathbf{u}_1, \mathbf{u}_2)\delta\left(\frac{r - \sigma}{\sigma}\right), \quad (3)$$

where f and Γ are functions yet to be determined, with $\Gamma \neq 0$ only for colliding particles with $(\mathbf{u}_2 - \mathbf{u}_1) \cdot \mathbf{r} < 0$. The extra δ contribution in Eq. (3) expresses that, when a particle collides on another, it skids along at contact for a finite amount of time as depicted in Fig. 1. In any dimension d (see [28]), the regular part f of the profile satisfies

$$-v_0(\mathbf{u}_2 - \mathbf{u}_1) \cdot \nabla_{\mathbf{r}} f + (\mathcal{R}f) = 0, \quad (4)$$

while the singular part Γ is a solution of

$$-v_0(\mathbf{u}_2 - \mathbf{u}_1) \cdot [f(\sigma\hat{\mathbf{r}}; \mathbf{u}_1, \mathbf{u}_2)\hat{\mathbf{r}} + \nabla_{\hat{\mathbf{r}}}\Gamma - (d-1)\Gamma\hat{\mathbf{r}}] + (\mathcal{R}\Gamma) = 0. \quad (5)$$

This equation expresses the flux balance of incoming particles on the obstacle with those leaving in the course of their skidding around. Given the scale separation between σ and the run length $\sqrt{d}\hat{v}_0\tau$, the contributions involving \mathcal{R} can safely be discarded as $d \rightarrow \infty$ in Eqs. (4) and (5). This allows us to obtain an exact expression for the functions f and Γ . Denoting, by θ , the angle between $\hat{\mathbf{r}}$ and $(\mathbf{u}_2 - \mathbf{u}_1)$, we obtain

$$g_0(\mathbf{0}, \mathbf{r}; \mathbf{u}_1, \mathbf{u}_2) = \Theta(r - \sigma)[1 - \Theta(\cos\theta)\Theta(\sigma - r \sin\theta)] + \Theta(-\cos\theta)\delta\left(\frac{d(r - \sigma)}{\sigma}\right). \quad (6)$$

For colliding particles ($\cos\theta < 0$), there is an accumulation at contact expressed by a delta peak. Since flipping while skidding does not occur in the infinite dimensional limit, there is a depletion of particles away from $r = \sigma$ (hence, the conditions $\cos\theta > 0$ and $\sigma - r \sin\theta > 0$ in the regular part). In practice, this depletion is felt over distances $r - \sigma = O(\sigma/d)$ (since $1 - \sin\theta \sim 1/d$) and, thus, bears no effect

beyond these scales. In arbitrary dimension, the dimensionless function Γ depends on the ratio $v_0\tau/\sigma$. As $d \gg 1$ this ratio goes to infinity and our final result for g_0 is, indeed, independent of the dynamical parameters v_0 and τ . The spatial distribution function eventually reads

$$g_0(r) = \frac{1}{\Omega_d^2} \int_{\mathbf{u}_1, \mathbf{u}_2} g_0(\mathbf{0}, \mathbf{r}; \mathbf{u}_1, \mathbf{u}_2) = \theta(r - \sigma) \left(1 + \frac{\sigma}{2} \delta(d(r - \sigma))\right), \quad (7)$$

where Ω_d is the solid angle in d dimensions. In the hard-sphere limit, products of the type $g_0(\mathbf{0}, \mathbf{r}; \mathbf{u}_1, \mathbf{u}_2)\nabla_{\mathbf{r}}V(\mathbf{r})$, which are found, e.g., in the virial formula for pressure, also converge to a well-defined distribution. From Eq. (2), we show (see [28]) that

$$\lim_{\text{hard sphere}} \int_{\sigma}^{+\infty} dr g_0(\mathbf{0}, \mathbf{r}; \mathbf{u}_1, \mathbf{u}_2) \partial_r V(r) = \frac{v_0}{2} [(\mathbf{u}_2 - \mathbf{u}_1) \cdot \hat{\mathbf{r}}] \Gamma(\hat{\mathbf{r}}; \mathbf{u}_1, \mathbf{u}_2). \quad (8)$$

The typical scaling of potential gradients $\partial_r V(r) \sim \hat{v}_0$ discussed earlier is now confirmed.

Now, we turn to the N -body problem. In the thermodynamic limit, we must deal with the infinite hierarchy of correlation functions inferred from the dynamics. Now, we sketch the argument that allows us to solve this hierarchy exactly in the $d \gg 1$ limit. This will lead us to conclude that the N -body two-point function $g^{(2)}$ actually reduces to g_0 determined in Eq. (6). The second equation of the hierarchy is given by

$$-v_0(\mathbf{u}_2 - \mathbf{u}_1) \cdot \nabla_{\mathbf{r}} g^{(2)} + (\mathcal{R}g^{(2)}) + 2\nabla_{\mathbf{r}} \cdot (g^{(2)} \nabla_{\mathbf{r}} V(\mathbf{r})) + \rho \nabla_{\mathbf{r}} \cdot \left(\int \frac{d\mathbf{u}'}{\Omega_d} d\mathbf{r}' (g^{(3)}(\mathbf{0}, \mathbf{r}, \mathbf{r}'; \mathbf{u}_1, \mathbf{u}_2, \mathbf{u}')) + g^{(3)}(\mathbf{0}, \mathbf{r}, \mathbf{r}'; -\mathbf{u}_1, -\mathbf{u}_2, \mathbf{u}') \nabla_{\mathbf{r}'} V(\mathbf{r}') \right) = 0, \quad (9)$$

and solving it requires, as usual, the knowledge of $g^{(3)}$. Assuming a truncation of the hierarchy at the level of the equation for $g^{(3)}$ itself, we show that the resulting equation for $g^{(2)}$ is that of the two-body system. This is at the basis of the systematic proof presented in [28]. The truncated equation for $g^{(3)}(\mathbf{0}, \mathbf{r}, \mathbf{r}'; \mathbf{u}_1, \mathbf{u}_2, \mathbf{u}')$ reads

$$-v_0(\mathbf{u}_2 - \mathbf{u}_1) \cdot \nabla_{\mathbf{r}} g^{(3)} - v_0(\mathbf{u}' - \mathbf{u}_1) \cdot \nabla_{\mathbf{r}'} g^{(3)} + (\mathcal{R}g^{(3)}) + \nabla_{\mathbf{r}} \cdot \{g^{(3)}[2\nabla_{\mathbf{r}} V(\mathbf{r}) + \nabla_{\mathbf{r}'} V(\mathbf{r}') + \nabla_{\mathbf{r}} V(\mathbf{r} - \mathbf{r}')]\} + \nabla_{\mathbf{r}'} \cdot \{g^{(3)}[2\nabla_{\mathbf{r}'} V(\mathbf{r}') + \nabla_{\mathbf{r}} V(\mathbf{r}) + \nabla_{\mathbf{r}'} V(\mathbf{r}' - \mathbf{r})]\} = 0. \quad (10)$$

This equation has the solution $g^{(3)}(\mathbf{0}, \mathbf{r}, \mathbf{r}'; \mathbf{u}_1, \mathbf{u}_2, \mathbf{u}') = g_0(\mathbf{0}, \mathbf{r}; \mathbf{u}_1, \mathbf{u}_2) g_0(\mathbf{0}, \mathbf{r}'; \mathbf{u}_1, \mathbf{u}') g_0(\mathbf{r}, \mathbf{r}'; \mathbf{u}_2, \mathbf{u}')$ up to $O(d^{-1/2})$

corrections. This structure is identical to the one encountered in equilibrium systems when truncating the hierarchy of correlations to the same order. It survives in the infinite-dimensional nonequilibrium steady state due to the amplitude of collision forces remaining $1/\sqrt{d}$ weaker than those of the self-propulsion ones and because the flipping term

$\mathcal{R}g^{(3)}$ is negligible. Now, we want to evaluate the last two terms in Eq. (9), which in the hard-sphere limit first requires us to regularize the product $g^{(3)}\nabla_{\mathbf{r}'}V(\mathbf{r}')$. In the same spirit as in Eq. (8), we can take the hard-sphere limit for $V(\mathbf{r}')$ [for now $V(\mathbf{r})$ and $V(\mathbf{r}' - \mathbf{r})$ are kept short-ranged and regular] and we find, using Eq. (10), that

$$\lim_{\text{hard sphere}} 2 \int_{\sigma}^{+\infty} dr' g^{(3)} \partial_{\mathbf{r}'} V(r') = [v_0(\mathbf{u}' - \mathbf{u}_1) - \nabla_{\mathbf{r}} V(\mathbf{r}) - \nabla_{\mathbf{r}'} V(\mathbf{r}' - \mathbf{r})] \cdot \hat{\mathbf{r}}' \lim_{x \rightarrow 0^+} \int_{\sigma}^{(1+x)\sigma} dr' g^{(3)}, \quad (11)$$

which holds irrespective of the $d \gg 1$ limit. We will now substitute our result for $g^{(3)}$ in terms of g_0 into Eq. (9) using Eq. (11) first. From the geometrical argument of [4], configurations with three particles at contact are exponentially rare as $d \rightarrow \infty$ (see also [28]). If $r - \sigma = O(\sigma/d)$, which is the domain of interest of Eq. (9), and given that $r' = \sigma$, we know that $(\|\mathbf{r} - \mathbf{r}'\|/\sigma) - 1 = O(1)$ except in an exponentially small fraction of the volume over which \mathbf{r}' is integrated. Thus, it is safe to set $\nabla_{\mathbf{r}} V(\mathbf{r} - \mathbf{r}') = \mathbf{0}$ and $g_0(\mathbf{r}, \mathbf{r}'; \mathbf{u}_2, \mathbf{u}') = 1$ in Eq. (9). This leads to

$$\begin{aligned} & \rho \left\{ \int \frac{d\mathbf{u}'}{\Omega_d} d\mathbf{r}' g^{(3)}(\mathbf{0}, \mathbf{r}, \mathbf{r}'; \mathbf{u}_1, \mathbf{u}_2, \mathbf{u}') \nabla_{\mathbf{r}'} V(\mathbf{r}') \right\} \\ &= -\frac{\rho V_d(\sigma)}{4d} g_0(\mathbf{0}, \mathbf{r}; \mathbf{u}_1, \mathbf{u}_2) [v_0 \mathbf{u}_1 + \nabla_{\mathbf{r}} V(\mathbf{r})] \left[1 + O(d^{-1/2}) \right], \end{aligned} \quad (12)$$

which, in turn, enforces $g^{(2)} = g_0$ up to $O(d^{-1/2})$ corrections as claimed in our introduction. This analytically supports the relevance of the Baxter model [35] as a proxy for analyzing the structure of active fluids as suggested in [36]. In addition, as shown in [28], the pair product structure extends to n -point distributions

$$g^{(n)}(\mathbf{r}_1, \dots, \mathbf{r}_n; \mathbf{u}_1, \dots, \mathbf{u}_n) = \prod_{i < j} g_0(\mathbf{r}_i, \mathbf{r}_j; \mathbf{u}_i, \mathbf{u}_j), \quad (13)$$

up to $O(d^{-1/2})$ corrections. For the three-body function, this shows that the Kirkwood approximation (used in $d = 2$ in [37]) becomes exact in infinite dimension. We are now in a position to determine the effective self-propulsion velocity of a tagged particle as introduced in [26]. From the equation of motion (1) averaged at given \mathbf{u}_i , we define $v(\rho)$ with $(d\langle \mathbf{r}_i \rangle_i / dt) = v(\rho) \mathbf{u}_i$, so that

$$v(\rho) = v_0 - \frac{\rho}{\Omega_d} \int_{\mathbf{u}_j, \mathbf{r}_j} g^{(2)}(\mathbf{r}_i, \mathbf{r}_j; \mathbf{u}_i, \mathbf{u}_j) \nabla_{\mathbf{r}_j} V(\mathbf{r}_i - \mathbf{r}_j) \cdot \mathbf{u}_i. \quad (14)$$

Using our result for $g^{(2)}$, Eq. (6), and Eq. (8), we arrive at a central result of this Letter

$$v(\rho) = v_0 \left(1 - \frac{\rho}{\rho_{\text{cr}}} \right), \quad \rho_{\text{cr}} = \frac{4d}{V_d(\sigma)}. \quad (15)$$

This immediately defines the range of validity of our calculation, such that $\rho < \rho_{\text{cr}}$. Indeed, $\rho > \rho_{\text{cr}}$ leads to a negative $v(\rho)$, which is unphysical, so that for $\rho > \rho_{\text{cr}}$ the system cannot be, at a microscopic level, in a homogeneous state, which echoes the findings of [38,39] in two-dimensional systems. The crowding density ρ_{cr} which controls this transition, is a density scale independent of the dynamical parameters v_0 and τ . In the analysis of existing numerical simulations, a linear function $v(\rho)$ has appeared to be an excellent fit both in two and three dimensions [24,27,40]. Numerics also show the vanishing of $v(\rho)$ beyond a threshold that was observed to be independent of dynamical parameters [27]. We conjecture that this arrest density is the crowding density ρ_{cr} of our calculation. Our large-dimensional prediction is that the transition occurs at a volume fraction $\phi = \rho V_d(\sigma/2) = 4d2^{-d}$ which is smaller than the corresponding jamming density of hyperspheres (which goes as $6.26d2^{-d}$ [12] for $d \gg 1$). Paradoxically, even though the crowding threshold depends on geometry only, it is tempting to view it as a new, intrinsically dynamical, jamming scale. Finally, considering the relative motion of two particles, the quantity $v(\rho)$ not only describes their effective self-propulsion velocity, but, surprisingly it also controls their effective mobility by reducing the amplitude of their direct interaction. Indeed, at given i and j self-propulsion velocities and positions,

$$\frac{d}{dt} \langle \mathbf{r}_i - \mathbf{r}_j \rangle_{ij} = v(\rho) (\mathbf{u}_i - \mathbf{u}_j) - 2 \frac{v(\rho)}{v_0} \nabla_{\mathbf{r}_i} V(\mathbf{r}_i - \mathbf{r}_j), \quad (16)$$

after making use of Eq. (12). Another interesting property of active particles interacting with pairwise forces is the existence of an equation of state for the pressure P , in the sense that it only depends on bulk properties of the fluid. Following [27], the pressure in a homogeneous state is given by

$$\begin{aligned} P &= \rho \frac{v_0^2 \tau v(\rho)}{d - v_0} \\ &- \frac{\rho^2}{2d\Omega_d^2} \int_{\mathbf{r}, \mathbf{u}_1, \mathbf{u}_2} g^{(2)}(\mathbf{0}, \mathbf{r}; \mathbf{u}_1, \mathbf{u}_2) \mathbf{r} \cdot \partial_{\mathbf{r}} V(\mathbf{r}). \end{aligned} \quad (17)$$

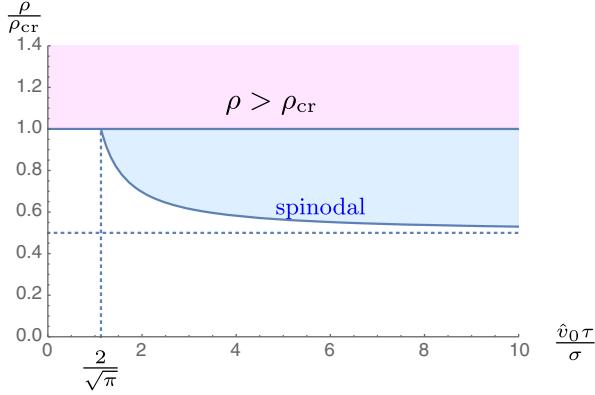


FIG. 2. Phase boundaries of a system of active hard spheres in infinite dimensions in the $(\hat{v}_0\tau/\sigma, \rho/\rho_{\text{cr}})$ plane. Magenta: Spinodal region for $\rho < \rho_{\text{cr}}$. Blue: $\rho > \rho_{\text{cr}}$ crowded region.

When $\rho < \rho_{\text{cr}}$, we have

$$\frac{P}{\sigma\rho_{\text{cr}}\hat{v}_0} = \frac{\hat{v}_0\tau}{\sigma} \frac{\rho}{\rho_{\text{cr}}} \left(1 - \frac{\rho}{\rho_{\text{cr}}}\right) + \frac{1}{\sqrt{\pi}} \frac{\rho^2}{\rho_{\text{cr}}^2}. \quad (18)$$

This exact equation of state is consistent with numerical observations [27]. It allows for spinodal instability when $\rho < \rho_{\text{cr}}$ and $(dP/d\rho) < 0$, hence, for $\hat{v}_0\tau > 2\sigma/\sqrt{\pi}$ (in line with the numerical observation [40] that the instability threshold for the run length increases with dimension). When this criterion is fulfilled, the spinodal region is defined by

$$1 > \frac{\rho}{\rho_{\text{cr}}} > \frac{1}{2} \frac{\sqrt{\pi} \hat{v}_0\tau / \sigma}{\sqrt{\pi} \hat{v}_0\tau / \sigma - 1}. \quad (19)$$

The spinodal boundaries of the phase diagram are shown in Fig. 2. Below ρ_{cr} , they are consistent with the findings presented in [38–41]. In infinite dimensions, we find the $\rho > \rho_{\text{cr}}$ region to overlap the phase separated region, a feature which also seems to emerge in the large $v_0\tau/\sigma$ corner of the phase diagram in [39].

The important results of this Letter are threefold. (i) There exists an infinite-dimensional limit in which the stationary properties of self-propelled particles interacting via a pairwise potential can be solved exactly. In the hard-sphere limit, the pair distribution function is shown to pick up a strongly attractive term at contact (in the form of a δ contribution). (ii) The effective self-propulsion velocity dressed by the interactions with other particles vanishes at a crowding density slightly smaller than the jamming one. Neither the pair distribution function nor the crowding density depend on the bare self-propulsion velocity or on the time scale governing the decay of self-propulsion correlations. (iii) These findings allow us to obtain the equation of state for self-propelled hard spheres in the homogeneous phase, and to find the location of the spinodal preempting MIPS. The range of directions our work opens up is manifold. First, as for their equilibrium

counterparts, active hard spheres in contact with a hard wall are characterized by a fluid-solid surface tension, the determination of which involves not only the pair distribution function [42,43] (computed in the present work in the large d limit), but also the density profile in the vicinity of the wall (in the spirit of [44]). Studying such a system in infinite dimension will allow us to gain insight into the interplay between the bulk and the near-wall physics of interacting active particles systems. Second, it is well known that, in equilibrium, the details of the dynamics bear no influence on the stationary properties; this is, of course, not so out of equilibrium. Here, we have studied the simplest instance of self-propelled dynamics, but hydrodynamic interactions could be incorporated, e.g., in the form of an Oseen motility tensor (see [45] for a d -dimensional version). Third, in the spirit of [46], the study of self-propelled rods in which alignment interactions will now introduce an additional physical ingredient. We sense, however, that equally interesting, though more involved, research directions lie in exploring the vicinity of the crowding density (at, and beyond [38,39]) and in capturing dynamical evolution [18], allowing us to access slow dynamics properties [47,48].

We acknowledge very insightful exchanges with L. Berthier, M. E. Cates, D. Limmer, K. Mandadapu, and J. Tailleur.

-
- [1] J.-P. Hansen and I. R. McDonald, *Theory of Simple Liquids* (Elsevier, Academic Press, 1990).
 - [2] J. E. Mayer and M. G. Mayer, *Statistical Mechanics*, 2nd ed. (Wiley, New York, 1977).
 - [3] J. S. Rowlinson, *Cohesion: A Scientific History of Intermolecular Forces* (Cambridge University Press, Cambridge, England, 2005).
 - [4] H. L. Frisch, N. Rivier, and D. Wyler, *Phys. Rev. Lett.* **54**, 2061 (1985).
 - [5] D. Wyler, N. Rivier, and H. L. Frisch, *Phys. Rev. A* **36**, 2422 (1987).
 - [6] H. L. Frisch and J. K. Percus, *Phys. Rev. E* **60**, 2942 (1999).
 - [7] Y. Elskens and H. L. Frisch, *Phys. Rev. A* **37**, 4351 (1988).
 - [8] H. L. Frisch and J. K. Percus, *Phys. Rev. A* **35**, 4696 (1987).
 - [9] R. Evans, *Adv. Phys.* **28**, 143 (1979).
 - [10] H. Löwen, in *Statistical Physics and Spatial Statistics*, edited by K. R. Mecke and D. Stoyan (Springer, Berlin, 2000), pp. 295–331.
 - [11] G. Parisi and F. Zamponi, *J. Stat. Mech.* (2006) P03017.
 - [12] G. Parisi and F. Zamponi, *Rev. Mod. Phys.* **82**, 789 (2010).
 - [13] J. Kurchan, G. Parisi, and F. Zamponi, *J. Stat. Mech.* (2012) P10012.
 - [14] A. Ikeda and K. Miyazaki, *Phys. Rev. Lett.* **104**, 255704 (2010).
 - [15] B. Schmid and R. Schilling, *Phys. Rev. E* **81**, 041502 (2010).
 - [16] T. Maimbourg, J. Kurchan, and F. Zamponi, *Phys. Rev. Lett.* **116**, 015902 (2016).

- [17] J. Kurchan, T. Maimbourg, and F. Zamponi, *J. Stat. Mech.* (2016) 033210.
- [18] E. Agoritsas, T. Maimbourg, and F. Zamponi, *J. Phys. A* **52**, 144002 (2019).
- [19] C. L. Hicks, M. J. Wheatley, M. J. Godfrey, and M. A. Moore, *Phys. Rev. Lett.* **120**, 225501 (2018).
- [20] S. Ramaswamy, *Annu. Rev. Condens. Matter Phys.* **1**, 323 (2010).
- [21] M. C. Marchetti, J. F. Joanny, S. Ramaswamy, T. B. Liverpool, J. Prost, M. Rao, and R. A. Simha, *Rev. Mod. Phys.* **85**, 1143 (2013).
- [22] É. Fodor and M. C. Marchetti, *Physica (Amsterdam)* **504A**, 106 (2018).
- [23] J. Tailleur and M. E. Cates, *Phys. Rev. Lett.* **100**, 218103 (2008).
- [24] Y. Fily and M. C. Marchetti, *Phys. Rev. Lett.* **108**, 235702 (2012).
- [25] G. S. Redner, M. F. Hagan, and A. Baskaran, *Phys. Rev. Lett.* **110**, 055701 (2013).
- [26] J. Bialké, H. Löwen, and T. Speck, *Europhys. Lett.* **103**, 30008 (2013).
- [27] A. P. Solon, J. Stenhammar, R. Wittkowski, M. Kardar, Y. Kafri, M. E. Cates, and J. Tailleur, *Phys. Rev. Lett.* **114**, 198301 (2015).
- [28] See Supplemental Material at <http://link.aps.org/supplemental/10.1103/PhysRevLett.123.260602> for further discussion and further mathematical details.
- [29] M. E. Cates and J. Tailleur, *Annu. Rev. Condens. Matter Phys.* **6**, 219 (2015).
- [30] G. Szamel, *Phys. Rev. E* **90**, 012111 (2014).
- [31] T. Maimbourg and J. Kurchan, *Europhys. Lett.* **114**, 60002 (2016).
- [32] P. Charbonneau, J. Kurchan, G. Parisi, P. Urbani, and F. Zamponi, *Annu. Rev. Condens. Matter Phys.* **8**, 265 (2017).
- [33] A. B. Slowman, M. R. Evans, and R. A. Blythe, *Phys. Rev. Lett.* **116**, 218101 (2016).
- [34] K. Malakar, V. Jemseena, A. Kundu, K. V. Kumar, S. Sabhapandit, S. N. Majumdar, S. Redner, and A. Dhar, *J. Stat. Mech.* (2018) 043215.
- [35] R. J. Baxter, *J. Chem. Phys.* **49**, 2770 (1968).
- [36] F. Ginot, I. Theurkauff, D. Levis, C. Ybert, L. Bocquet, L. Berthier, and C. Cottin-Bizonne, *Phys. Rev. X* **5**, 011004 (2015).
- [37] A. Härtel, D. Richard, and T. Speck, *Phys. Rev. E* **97**, 012606 (2018).
- [38] J. U. Klamser, S. C. Kapfer, and W. Krauth, *Nat. Commun.* **9**, 5045 (2018).
- [39] P. Digregorio, D. Levis, A. Suma, L. F. Cugliandolo, G. Gonnella, and I. Pagonabarraga, *Phys. Rev. Lett.* **121**, 098003 (2018).
- [40] J. Stenhammar, D. Marenduzzo, R. J. Allen, and M. E. Cates, *Soft Matter* **10**, 1489 (2014).
- [41] D. Levis, J. Codina, and I. Pagonabarraga, *Soft Matter* **13**, 8113 (2017).
- [42] A. Bellemans, *Physica* **28**, 493 (1962).
- [43] R. Zakine, Y. Zhao, M. Knezevic, A. Daerr, Y. Kafri, J. Tailleur, and F. van Wijland (to be published).
- [44] B. Ezhilan, R. Alonso-Matilla, and D. Saintillan, *J. Fluid Mech.* **781**, R4 (2015).
- [45] B. Charbonneau, P. Charbonneau, Y. Jin, G. Parisi, and F. Zamponi, *J. Chem. Phys.* **139**, 164502 (2013).
- [46] H.-O. Carmesin, H. L. Frisch, and J. K. Percus, *Phys. Rev. B* **40**, 9416 (1989).
- [47] R. Ni, M. A. C. Stuart, and M. Dijkstra, *Nat. Commun.* **4**, 2704 (2013).
- [48] L. Berthier, E. Flenner, and G. Szamel, *J. Chem. Phys.* **150**, 200901 (2019).